

Keywords: colorectal cancer; ulcerative colitis; IL-6; STAT3; GADD34; myeloid cells

Effects of growth arrest and DNA damage-inducible protein 34 (GADD34) on inflammation-induced colon cancer in mice

Yuriko Tanaka¹, Sachiko Ito¹, Reina Oshino¹, Nana Chen¹, Naomi Nishio¹ and Ken-ichi Isobe^{*,1}

¹Department of Immunology, Nagoya University Graduate School of Medicine, 65 Tsurumai-cho, Showa-ku, Nagoya, Aichi 466-8550, Japan

Background: Growth arrest and DNA damage-inducible protein 34 (GADD34/Ppp1r15a) is a family of GADD proteins that are induced by DNA damage. GADD34 protein has been suggested to regulate inflammation or host defense systems. However, the *in vivo* function of GADD34 in inflammation is still unclear. Long lasting inflammation, such as that seen in Crohn's disease and ulcerative colitis, is associated with a higher incidence of colorectal cancer (CRC).

Methods: Using a colitis-associated cancer model, we analysed GADD34-deficient (KO) mice to study the effect of GADD34 on colitis and colorectal tumorigenesis.

Results: We found a higher incidence of CRC in wild-type (WT) mice than in GADD34KO mice. Moreover, dextran sodium sulfate (DSS)-induced inflammatory responses were downregulated by GADD34 deficiency. The expression of pro-inflammatory mediators such as TNF α , IL-6, and iNOS/NOS2 was higher in the colons of WT mice than GADD34KO mice. IL-6 is known to activate STAT3 signalling in colonic epithelial cells and subsequently induced epithelial proliferation. We found that IL-6-STAT3 signalling and epithelial proliferation were higher in WT mice compared with GADD34KO mice.

Conclusions: These results indicated that GADD34 upregulated pro-inflammatory mediator production leading to a higher tumour burden following azoxymethane (AOM)/DSS treatment.

Colorectal cancer (CRC) is the third most common cancer and it is suspected to be linked to the western lifestyle. Indeed, the incidence for CRC in high-income countries such as United States, Japan, and Western Europe is 10-fold higher than that in low-income and middle-income countries (Jemal *et al*, 2010). Environmental factors that induce inflammation have been suggested to augment the growth of CRC. In the human gut, there are approximately 10¹³ commensal bacteria dominated by *Bacteroidetes*, *Firmicutes*, and *Proteobacteria* (Arumugam *et al*, 2011). It has been suggested that imbalances in these bacterial populations may cause colitis that in turn proceeds to CRC. Indeed, long lasting inflammatory processes such as that found in Crohn's disease and ulcerative colitis are associated with a higher incidence of CRC (Jemal *et al*, 2010; Herrinton *et al*, 2012).

Growth arrest and DNA damage-inducible protein 34 (GADD34/Ppp1r15a) was originally isolated based on ultraviolet-inducible transcripts in Chinese hamster ovary cells (Arumugam *et al*, 2011). It belongs to a family of GADD genes that are induced by DNA damage (Zhan *et al*, 1994). Expression of GADD34 is also induced by amino-acid deprivation and several types of endoplasmic reticulum (ER) stresses (Mengesdorf *et al*, 2001; Novoa *et al*, 2001; Ito *et al*, 2015). Hollander *et al* (1997) demonstrated a correlation between the onset of apoptosis and GADD34 expression in selected cell lines following ionising irradiation or treatment with the alkylating agent methyl methanesulfonate. Later, GADD34 was shown to dephosphorylate several kinases that function in important signalling cascades. Two related genes, Ppp1r15a and Ppp1r15b, encoding the proteins GADD34 and

*Correspondence: Dr K Isobe; E-mail: kisobe@med.nagoya-u.ac.jp

Received 9 February 2015; revised 7 May 2015; accepted 24 June 2015

© 2015 Cancer Research UK. All rights reserved 0007–0920/15

CREP, respectively, recruit a catalytic subunit from one of several related protein phosphatase I (PP1) isoforms to form a holophosphatase complex that can dephosphorylate several enzymes *in vitro* (Harding *et al*, 2009). Using GADD34-deficient (KO) mice, our laboratory and others have shown that GADD34 dephosphorylates the translation initiation factor eIF2 α and inhibits the shut-off of protein translation (Kojima *et al*, 2003; Novoa *et al*, 2003). Furthermore, GADD34-PP1 dephosphorylates several signalling molecules that are engaged in inflammation or the host defense system. Viral or bacterial infections are affected by GADD34 including vesicular stomatitis virus (Herrinton *et al*, 2012) and measles virus infection (Fornace *et al*, 1988; Mesman *et al*, 2014). GADD34 dephosphorylates IKK β (Li *et al*, 2008) and Tak1 (Gu *et al*, 2014), which affect inflammatory signalling.

Because GADD34 contributes to apoptosis, ER stresses, and inflammation, we hypothesised that GADD34 could modify tumour initiation and inflammatory carcinogenesis. However, whether GADD34 would enhance or suppress tumour initiation and inflammation was unclear. To test this hypothesis, the azoxymethane/dextran sodium sulfate (AOM/DSS) system is ideal because AOM/DSS models have been widely used to study inflammation-dependent CRC (Becker *et al*, 2004; Greten *et al*, 2004). Here, we investigated the murine inflammatory colitis AOM/DSS model in GADD34KO mice.

MATERIALS AND METHODS

Mice. All experiments used 6- to 8-week-old wild-type (WT) and GADD34-deficient (GADD34KO) female mice born from the same mother, and maintained at the Animal Research Facility at Nagoya University Graduate School of Medicine under specific pathogen-free conditions. GADD34KO mice were generated as previously described (Kojima *et al*, 2003). Originally, GADD34KO mice were produced from ES cells with a C57BL/6 and 129 background. These mice were backcrossed to WT for up to 10 generations. This work was approved by the ethical committee of Nagoya University.

Induction of CRC. Mice were intraperitoneally injected with 12 mg kg⁻¹ body weight of AOM (Sigma-Aldrich, St Louis, MO, USA) dissolved in phosphate-buffered saline (PBS). Five days after AOM administration, 2% DSS (MP Biomedicals, Santa Ana, CA, USA, molecular weight 35 000–50 000 kDa) was administered in the drinking water for 5 consecutive days (first round of DSS treatment). Subsequently, untreated water was given for 16 days. Then DSS was administered for 5 days followed by 16 days of pure water (second round of DSS treatment). Finally, DSS was administered for 4 days (third round of DSS treatment) (Figure 1A). Body weight was assessed at least 3 days per week throughout the course of the experiment.

DSS-induced colitis model. Acute colitis was induced with 2% DSS for 5 days followed by normal drinking water until the end of the experiment (Figure 2A).

Histopathological analysis. Mouse colon tissues were prepared as Swiss rolls, fixed in 4% paraformaldehyde in neutral buffer solution for paraffin embedding. Paraffin-embedded tissues were cut into 4- μ m sections and stained with haematoxylin and eosin (H&E). Histology scores were determined as described in a previous report (Zaki *et al*, 2011). These scores were assigned as follows, based on the extent and severity of inflammation, ulceration, and hyperplasia of the mucosa in the distal colon.

Inflammation: 0 = normal; 1 = mild (small, focal, or widely separated, limited to the lamina propria); 2 = moderate (multi-focal or locally extensive, extending to submucosa); 3 = severe (transmural inflammation with ulcers covering > 20 crypts).

Ulceration: 0 = normal; 1 = mild (1 or 2 ulcers involving up to a total of 20 crypts); 2 = moderate (1 to 4 ulcers involving a total of 20–40 crypts); 3 = severe (> 4 ulcers or over 40 crypts).

Hyperplasia: 0 = normal; 1 = mild (crypts 2 to 3 times normal thickness, normal epithelium); 2 = moderate (crypts 2 to 3 times normal thickness, hyperchromatic epithelium, reduced goblet cells, scattered arborisation); 3 = severe (crypt > 4 times normal thickness, marked hyperchromasia, few to no goblet cells, high mitotic index, frequent arborisation).

Extent: 0 = normal (0% involvement); 1 = mild (up to 30% involvement); 2 = moderate (30–70% involvement); 3 = severe (over 70% involvement).

Real-time PCR analysis. Total RNA was isolated using an RNeasy mini kit (Qiagen, Hilden, Germany) according to the manufacturer's recommended protocol. Residual genomic DNA was digested and removed using DNase I (Invitrogen, Waltham, MA, USA) treatment. First-strand cDNA was synthesised using 1 μ g total RNA and a High Capacity cDNA Reverse Transcription Kit (Applied BioSystems, Waltham, MA, USA) for real-time PCR. Real-time PCR was performed using SYBR green (Toyobo, Osaka, Japan) according to the manufacturer's instructions. Expression data were normalised to *Gapdh* mRNA expression. The primer sequences are shown in Supplementary Table 1.

Cytokines from serum and supernatants from cultured colon tissue. Serum samples and distal colons were taken from naïve or DSS-treated WT and GADD34KO mice. Colon tissues were cultured in serum-free RPMI medium containing penicillin/streptomycin for 24 h and cultured supernatants were collected. IL-6 and TNF α protein in serum and in cultured colon supernatants was determined by specific ELISA kits according to the manufacturer's instructions (R&D Systems, Minneapolis, NE, USA).

Western blot analysis and immunohistochemistry. Tissue samples were homogenised in standard RIPA buffer with PMSF. The protein concentration was determined with a DC Protein Assay Kit (Bio-Rad, Hercules, CA, USA). Lysates (30 μ g protein) were separated by 6–10% SDS-gel electrophoresis, and transferred onto PVDF membranes (Millipore, Darmstadt, Germany). Membranes were blocked in PBST buffer containing 3% skim milk for 1 h at room temperature, probed with primary antibodies and secondary HRP-conjugated antibodies (GE Healthcare, Little Chalfont, UK), and developed using the ECL Western blot detection reagents (GE Healthcare).

Paraffin-embedded slides were deparaffinised, and boiled in citrate buffer for antigen retrieval and stained overnight with anti-IL-6 (Abcam, Cambridge, UK; 1 : 400 dilution), anti-p-STAT3 (Cell Signaling, Danvers, MA, USA; 1 : 400 dilution) or anti-Ki67 (Santa Cruz, Santa Cruz, CA, USA; 1 : 200 dilution) antibodies. TUNEL staining was performed using an *In Situ* Apoptosis Detection Kit (Takara, Shiga, Japan). The TUNEL-stained slides were analysed with a Nikon A1RSi Laser Scanning Confocal Microscope (Nikon, Tokyo, Japan).

Immunofluorescence analysis. Colon tissues from mice were embedded in OCT compound (Sakura Finetek, Tokyo, Japan). Four-micrometer sections were fixed in 4% paraformaldehyde. After rinsing with PBS, sections were permeabilised and treated with blocking buffer (0.2% Triton X-100, 0.2% bovine serum albumin (BSA) and 0.1% normal goat serum in PBS). FITC-conjugated anti-IL-6 (eBioscience, Santa Clara, CA, USA), APC-conjugated anti-F4/80 (eBioscience) and Cy3-conjugated anti- α -SMA (Sigma-Aldrich) were used at 1 : 500 dilutions and incubated at 4 °C overnight, after which sections were washed with PBS and incubated with 4,6-diamidino-2-phenylindole (DAPI) for 5 min. After rinsing with PBS, the sections were mounted with mounting fluid and visualised under A1RSi inverted Confocal Microscopy (Nikon).

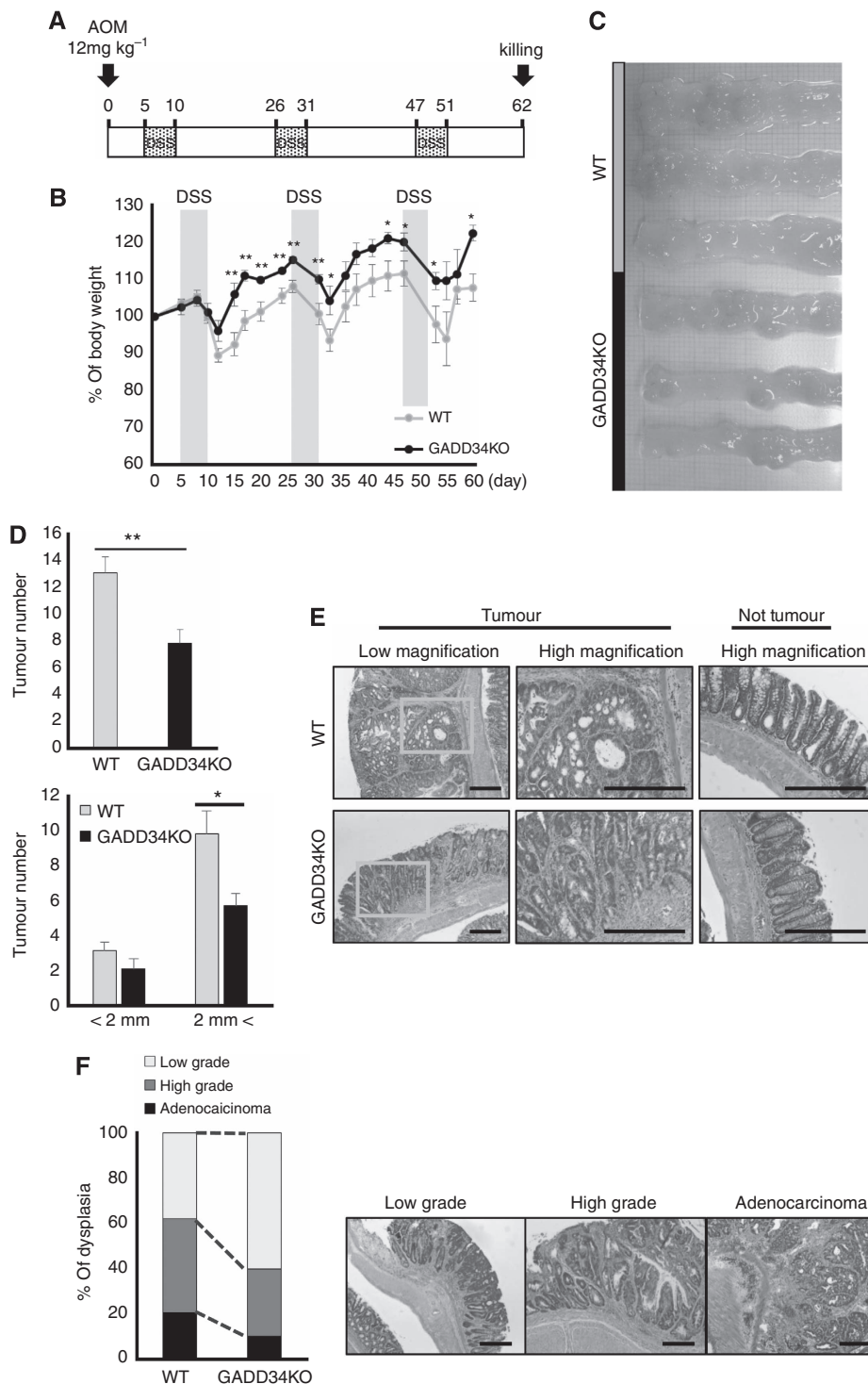


Figure 1. GADD34 promoted tumour formation in a mouse colitis-associated cancer model. (A) Schematic diagram of AOM/DSS-induced colitis-associated colon cancer model. (B) Body weight changes. Body weight at day 0 = 100%. Data represent means ± s.e.m. (n = 6). (C) After AOM injection, mice were killed on day 62 to determine tumour development in the colon. (D) Upper: Number of tumours in the whole colon (day 62). Lower: Number of small tumours (<2 mm) and large tumours (>2 mm) in the whole colon. (E) Representative images of H&E staining of tumours and normal regions. Scale bar: 300 μm. (F) Left: Overall grading of dysplasia in each genotype. Right: Representative high magnification images showing dysplasia in colon tissue. Scale bar: 300 μm. Data are means ± s.e.m. (WT: n = 10, GADD34KO: n = 8). *P < 0.05; **P < 0.01.

Lamina propria cell isolation. Colons were opened longitudinally, cut into fine pieces, and incubated with Hanks’ balanced salt solution (HBSS) containing 5 mM EDTA for 15 min at 37 °C to remove epithelial cells. Colonic pieces without epithelial cells were then incubated with PBS containing 4% fetal bovine serum (FBS), 0.5 mg ml⁻¹ collagenase typeII, 1 mg ml⁻¹ dispase and

50 μg ml⁻¹ DNase for 20 min at 37 °C. The cells were washed twice and suspended in PBS.

Flow-cytometric analyses and cell sorting. The cells were washed twice and cells (1 × 10⁶) were suspended in 50 μl PBS supplemented with 1% FBS and stained for 20 min at 4 °C with directly

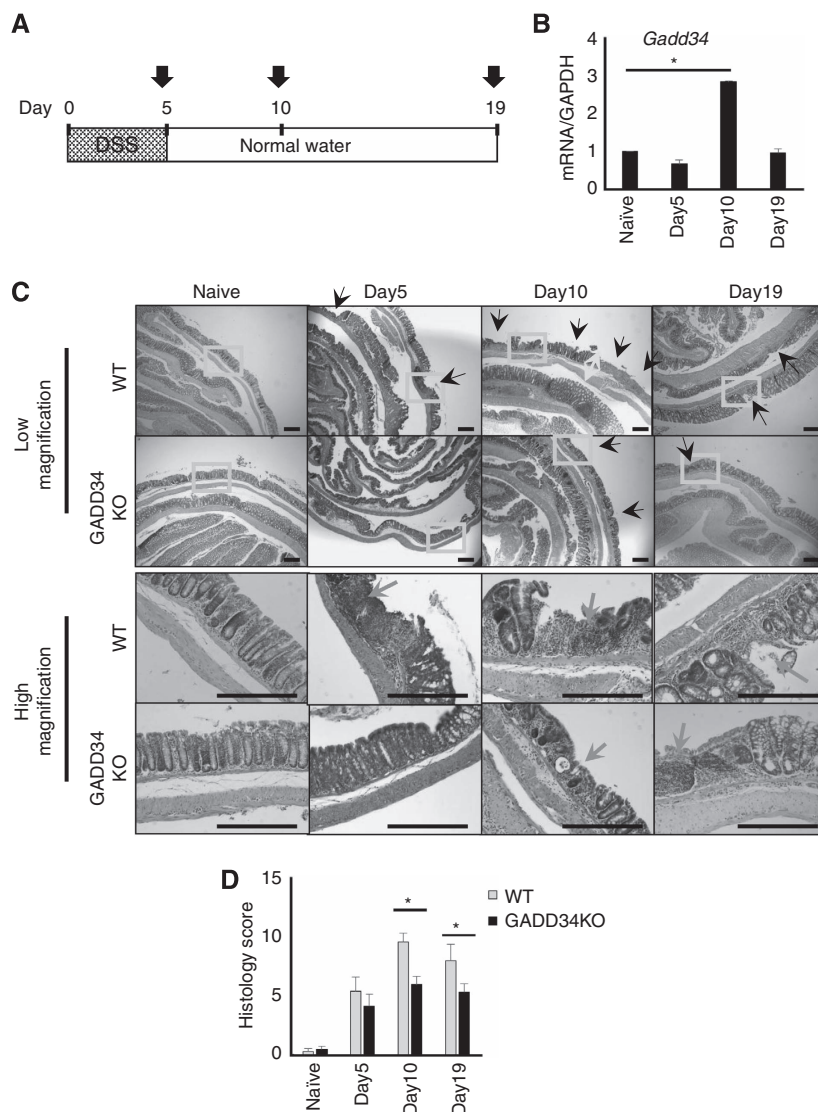


Figure 2. GADD34 increased the severity of experimental colitis. (A) Schematic diagram of mice treated with DSS. (B) Real-time PCR analysis for *Gadd34* mRNA in whole distal colon collected from WT mice at the indicated day. (C) Low magnification (upper) and high magnification (lower) of H&E staining of colon tissues taken from DSS-treated mice at days 0, 5, 10, and 19. Black arrows: ulceration, yellow arrows: hyperplasia, blue arrows: infiltration. Scale bar: 300 μ m. (D) Semiquantitative scoring of histopathology. Data represent means \pm s.e.m. ($n = 7$). * $P < 0.05$. A full color version of this figure is available at the *British Journal of Cancer* journal online.

conjugated fluorescent antibodies (1:500). Antibodies were as follows: eFluor450-conjugated anti-CD11b (eBioscience); FITC-conjugated anti-Gr-1 (BD Biosciences, Franklin Lakes, NJ, USA); APC-conjugated anti-Gr-1 (eBioscience); FITC-conjugated anti-CD11c (eBioscience). Stained cells were analysed with a FACS Canto flow cytometer using FACS Diva software (BD Biosciences), and the data were analysed with FlowJo software (TreeStar, Ashland, OR, USA). Cells were sorted with a FACS Aria flow cytometer (BD Biosciences) and washed twice and suspended in PBS. Cells (2×10^5) were resuspended in 100 μ l PBS and centrifuged onto microscope slides using a Cytospin-4 (Thermo Scientific, Waltham, MA, USA). Slides were then stained by May-Grunwald Giemsa according to a standard protocol.

Reactive oxygen species production analysis. Flow cytometry was used to measure intracellular reactive oxygen species (ROS) accumulation with 5-(and 6-)-chloromethyl-2',7'-dichlorodihydrofluorescein diacetate, acetyl ester (CM-H2DCFDA) (Invitrogen). Isolated lamina propria cells were incubated

in RPMI medium (Sigma-Aldrich) containing 5 μ M CM-H2DCFDA for 30 min at 37 $^{\circ}$ C in the dark. Fluorescence was analysed with a FACS Canto flow cytometer as described previously.

Statistical analyses. Data are expressed as means \pm standard error of the mean (s.e.m.). Differences were analysed by Student's *t*-test. *P*-values less than 0.05 were considered as statistically significant.

RESULTS

GADD34 promoted tumour formation in a mouse colitis-associated cancer model. To assess the role of GADD34 in tumour formation, WT and GADD34-deficient (GADD34KO) mice were treated with AOM and three rounds of DSS (Figure 1A). Changes in body weight were monitored three times per week throughout the study duration and colonic tumour burden was determined 62 days after AOM/DSS treatment. Body weight loss in

GADD34KO mice was significantly less than that in WT mice (Figure 1B). GADD34KO mice had a significantly lower tumour burden in the colon (Figure 1C and D), and the number of large tumours was lower than in WT mice (Figure 1D). We found that *Gadd34* gene expression was upregulated in the colon, especially epithelial cells of tumour-bearing mice (Supplementary Figure 1a and b). Histological examination of tumours was evaluated by staining. The tumour grade of WT mice was higher than that of GADD34KO mice (Figure 1E and F). About 60% of tumours were classified as high grade adenomas and adenocarcinomas in WT mice, and about 40% were classified as high grade adenomas and adenocarcinomas in GADD34KO mice (Figure 1F).

GADD34 increased the severity of experimental colitis. To investigate the role of GADD34 in colitis-induced inflammation, WT and GADD34KO mice were fed 2% DSS in drinking water for 5 days, after which they were given normal drinking water (Figure 2A). They were killed during the acute (day 5) and recovery (days 10 and 19) stages. *Gadd34* mRNA expression was significantly upregulated at day 10 (Figure 2B). Upregulation of *Gadd34* expression was detected in both immune cells and epithelial cells (Supplementary Figure 1c). Histopathological analysis revealed that WT mice had more severely damaged colonic mucosa, as evidenced by the loss of crypt structure and hyperplasia, larger areas of ulceration, and more extensive infiltration of inflammatory cells than GADD34 KO mice (Figure 2C and D).

GADD34 promoted epithelial growth through the IL-6-STAT3 axis. In WT colon, one round of DSS treatment led to immune cell infiltration and enhancement of mRNA expression for pro-inflammatory mediators, including *Il-6*, *Tnfr*, *Il-1 β* , and *Nos2/inos*. Expression of these genes was higher in WT mice than in GADD34KO mice (Figure 3A). IL-6 and TNF α protein levels in sera and cultured supernatants of colon tissue were also higher in WT mice than those in GADD34KO mice (Figure 3B and C). Strong iNOS/NOS2 protein expression was confirmed in WT mice but not in GADD34KO mice (Figure 3D and E). These results suggest that GADD34 increased the severity of experimental colitis through upregulating pro-inflammatory mediators.

Next, we examined NF κ B, STAT and MAPK signalling pathways that induce the expression of pro-inflammatory genes following one round of DSS. We observed high expression of p-STAT3 protein that correlated with IL-6 expression in WT mice (Figure 3D and E). The expression of p-STAT3 was lower in GADD34 KO mice than in WT mice. However, the expression of p-NF κ B p65 and p-I κ B α was not significantly different between WT and GADD34 KO mice (Figure 3D and E). On the other hand, we observed higher expression of members of the MAPK signalling pathway, p-ERK and p-JNK (46kDa) in WT mice than those in GADD34 KO mice (Figure 3F and G), although p-p38 expression was not increased by one round of DSS treatment in either WT or GADD34KO mice (Figure 3F and G).

We then asked whether immune cells and/or epithelial cells could produce pro-inflammatory cytokines. To solve the question, cells were assessed by immunohistochemistry for production of IL-6. We observed that IL-6 was mainly produced by infiltrating cells in DSS-treated mice. The expression of cytosolic IL-6 was higher in WT mice than in GADD34KO mice (Figure 4A). Using immunofluorescent staining, we found that IL-6 was mainly produced by F4/80-positive macrophages but not α -SMA-positive fibroblasts (Figure 4B). IL-6 may induce STAT3 signalling by binding to epithelial cells. We observed clear expression of p-STAT3 in colon epithelial cells. The expression of intracellular p-STAT3 was higher in WT mice than in GADD34KO mice (Figure 4C and D). Moreover, GADD34 promoted colon epithelial proliferation as detected by Ki-67 staining in the AOM/DSS-induced colitis model (Figure 4E and F).

GADD34 deficiency attenuated the recruitment of pro-inflammatory myeloid cells. The expression of inflammatory cytokines by immune cells indicated that myeloid cell infiltration was underway during DSS-induced colitis. DSS may damage colon epithelial cells, a process that can induce chemokines. Chemokine genes such as *Mcp1*, *Cxcl2*, and *Cxcr2* and *Csf3* (granulocyte-colony stimulating factor) were highly expressed in WT mice after DSS treatment. Expression of those genes was lower in GADD34 KO mice than in WT mice (Figure 5A). Gr-1^{high}/CD11b^{high} neutrophils and CD11b+/CD11c- macrophages were highly recruited to the colons of DSS-treated WT mice. Infiltration of these cells was less pronounced in GADD34KO colons (Figure 5B and C). In DSS-treated colon, myeloid cells produced ROS. The expression of ROS following DSS treatment was higher in WT mice than in GADD34KO mice (Figure 5D and E). We observed high ROS production in Gr-1^{high}/CD11b^{high} neutrophils (Figure 5F and G). Taken together, these results indicated that GADD34 had a critical role in promoting the inflammatory response following DSS-induced injury of the colonic epithelium.

Effect of GADD34 on AOM treatment. Next, we investigated the effect of GADD34 on the administration of AOM alone. Azoxymethane and its precursor compound 1, 2-dimethylhydrazine (DMH) are alkylating agents in the liver and colon. They cause DNA mutation by binding alkyl or methyl groups to guanine residues, resulting in G-to-A transition mutations (Dipple, 1995). Azoxymethane (12 mg kg⁻¹) was injected intraperitoneally into WT and GADD34KO mice. *Gadd34* mRNA expression was observed 24 h after AOM treatment (Supplementary Figure 2a). Histological examination 24 h after AOM administration revealed that the pathological changes were weak and no differences between WT and GADD34KO mice were detected (Supplementary Figure 2b). Because AOM induces DNA damage, we examined p-p53 expression. We found that the level of p-p53 was enhanced by the administration of AOM both in WT and in GADD34KO mice. The expression of p-p53 did not differ between WT and GADD34KO mice (Supplementary Figure 2c). We also examined the expression of p-eIF2 α (ER stress marker), p-NF κ B and p-STAT3 (inflammatory signalling) proteins. The expression of these proteins was not readily observed in either WT or GADD34KO mice (Supplementary Figure 2c). The expression levels of IL-6 (an inflammatory cytokine) and CHOP and ATF4 (ER stress markers) were slightly increased by the administration of AOM but there were no differences between WT and GADD34KO mice (Supplementary Figure 2d).

AOM/DSS treatment-induced inflammation. Finally, we examined the effects of GADD34 on AOM/DSS treatment. WT and GADD34KO mice were injected with 12 mg kg⁻¹ AOM and the animals were given normal drinking water. Five days after AOM treatment, they were fed 2% DSS for 5 days in drinking water after which they were given normal drinking water (Figure 6A). They were killed at day15, and the severity of colitis and pro-inflammatory mediator production was analysed. The loss of body weight was slightly greater in WT mice than in GADD34KO mice (Figure 6B). Compared with GADD34KO mice, WT mice had more severely damaged colonic mucosa, with loss of crypt structures and hyperplasia, larger areas of ulceration and more extensive infiltration of inflammatory cells (Figure 6C and D). In WT mice, AOM with one round of DSS treatment induced pro-inflammatory mediators (IL-6, TNF α , and iNOS/NOS2) but all of them were downregulated in GADD34KO mouse colons (Figure 6E). Additionally, GADD34 promoted colon epithelial proliferation as detected by Ki-67 staining in the AOM/DSS-induced colitis model (Figure 6F).

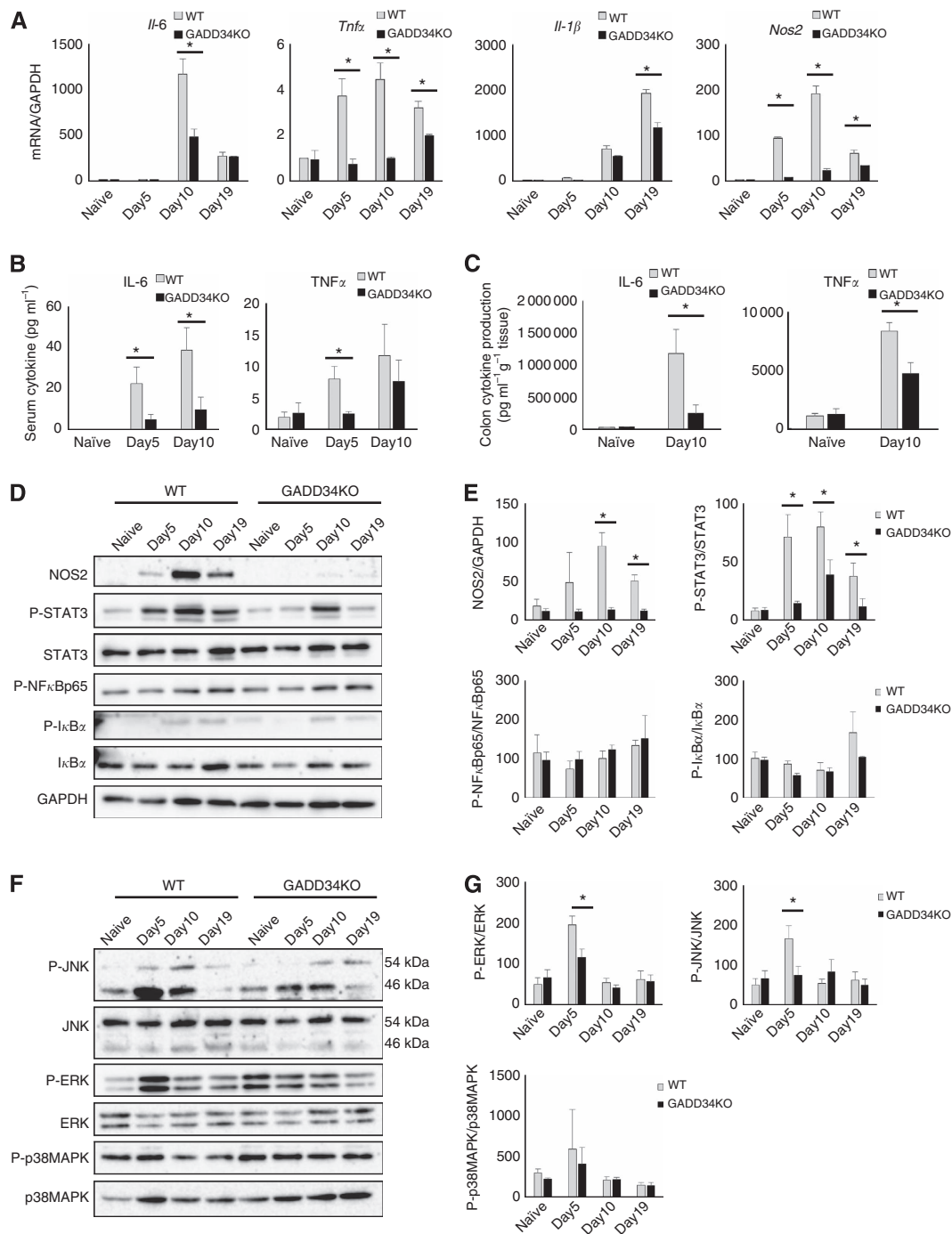


Figure 3. GADD34 regulated the production of pro-inflammatory mediators in experimental colitis. (A) Expression of pro-inflammatory mediator genes (*Il-6*, *Tnfx*, *Il-1β*, *Nos2/inos*) in whole distal colon was analysed by real-time PCR. **(B)** Serum cytokine levels (IL-6 and TNF α) were measured by ELISA. **(C)** Colon cytokine production (IL-6 and TNF α). Distal colons were taken from naïve or DSS-treated WT/GADD34KO mice and cultured in serum-free RPMI medium containing penicillin/streptomycin for 24h. The supernatants were assessed by ELISA. **(D–G)** Whole colon tissues collected at days 0, 5, 10, and 19 were processed for western blot analysis. Representative data are shown in **(D and F)**; quantitation of western blotting analysis is shown in **(E and G)**. Data represent means \pm s.e.m. ($n = 7$). $*P < 0.05$.

DISCUSSION

Here, we have shown that GADD34 expression enhanced CRC tumorigenesis. Moreover, we found that DSS-induced inflammatory responses were downregulated by GADD34 deficiency. Expression levels of pro-inflammatory cytokines such as TNF α , IL-6, and IL-1 β were higher in WT mice than in GADD34KO mice. Inflammatory conditions have been shown to promote oncogene

transformation and tumour progression (Mantovani *et al*, 2008). It is particularly interesting that IL-6 was continuously expressed in the colon during the course of AOM/DSS treatment. A correlation between IL-6 levels and the clinical activity of inflammatory bowel disease (IBD) and CRC has been demonstrated (Atreya and Neurath, 2005). IL-6 binds to its receptor (IL-6R α) that in turn interacts with gp130 and activates Janus kinases (JAK) and STAT3 (Kishimoto, 2005). The IL-6/STAT3 cascade is an important regulator of the proliferation of tumour cells (Grivennikov *et al*,

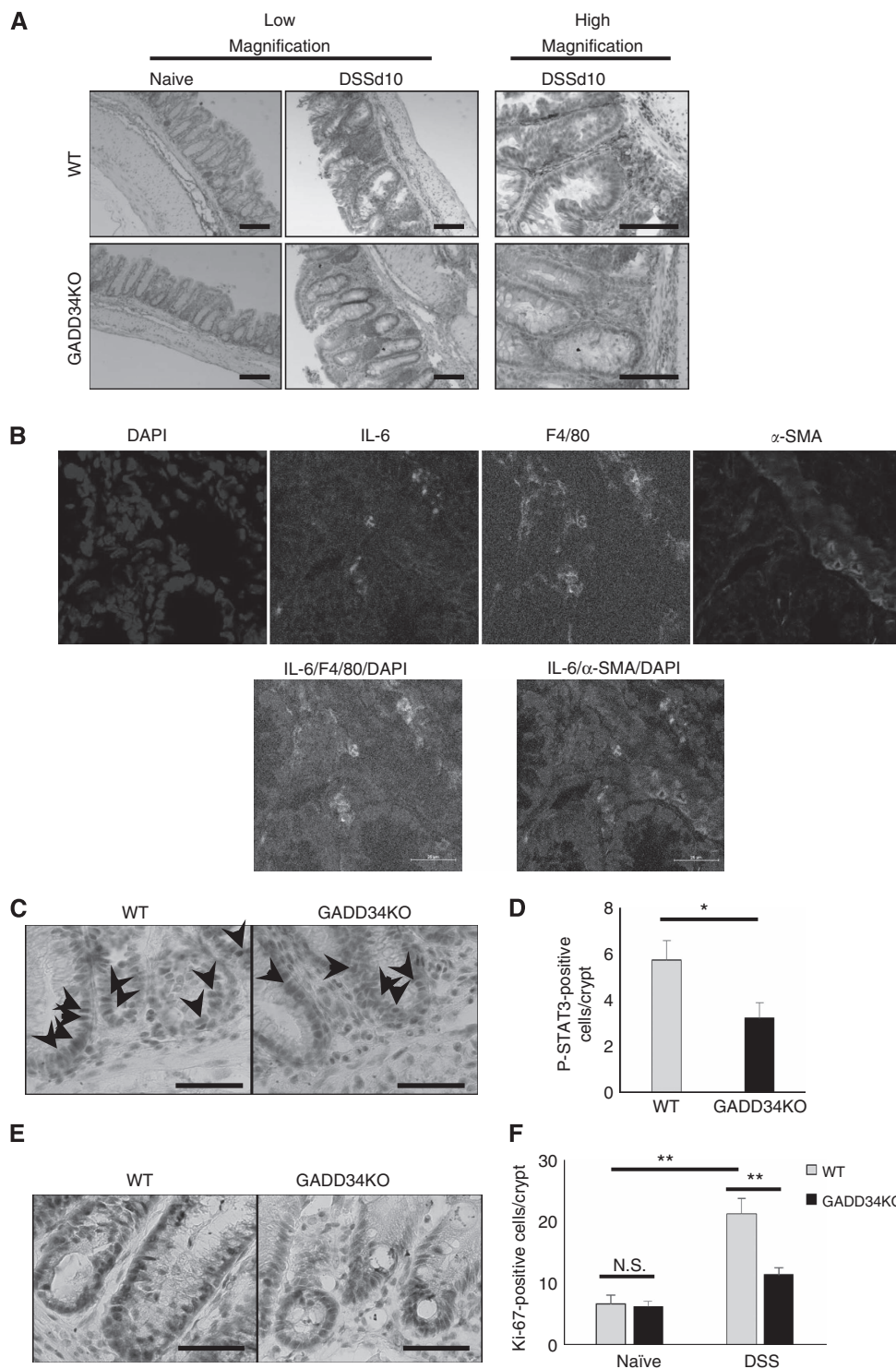


Figure 4. GADD34 promoted colon epithelium growth through upregulating IL-6 production. (A) Distal colons from DSS-treated mice (day 10) of both genotypes were stained with anti-IL-6. Scale bars: 100 μ m (B) Immunofluorescence analysis of DSS-treated WT mice. Blue: DAPI, Green: IL-6, Pink: F4/80 (macrophages), Red: α -SMA (fibroblasts). Scale bar: 25 μ m. (C–F) Distal colons from DSS-treated mice (day 10) of both genotypes were stained with anti-p-STAT3 (C) and anti-Ki-67 antibodies (E). Scale bar: 50 μ m (C and E). Black arrows show p-STAT3-positive intestinal epithelial cells (C). Number of p-STAT3-positive epithelial cells (D) and Ki-67-positive cells (F) were counted 10 days after DSS treatment. Data represent means \pm s.e.m. ($n = 6$). * $P < 0.05$, ** $P < 0.01$. A full color version of this figure is available at the *British Journal of Cancer* journal online.

2009; Yu *et al*, 2009). It was recently shown that TLRs are expressed by gut epithelial cells, and they induce protective roles against microbes, including the production of pro-inflammatory cytokines (Abreu, 2010). We identified the main cells that produced pro-inflammatory cytokines following the administration of DSS. Specifically, we showed here that DSS treatment

induced IL-6 production in myeloid cells that migrated to the DSS-damaged colonic tissue. Further, we found that p-STAT3 was expressed in DSS-damaged colonic epithelial cells. These expression levels were higher in WT mice than in GADD34KO mice. In fact, not only IL-6, but also TNF α , IL-1 β , and NO production was greatly enhanced in WT mice. In the DSS colitis model, NO

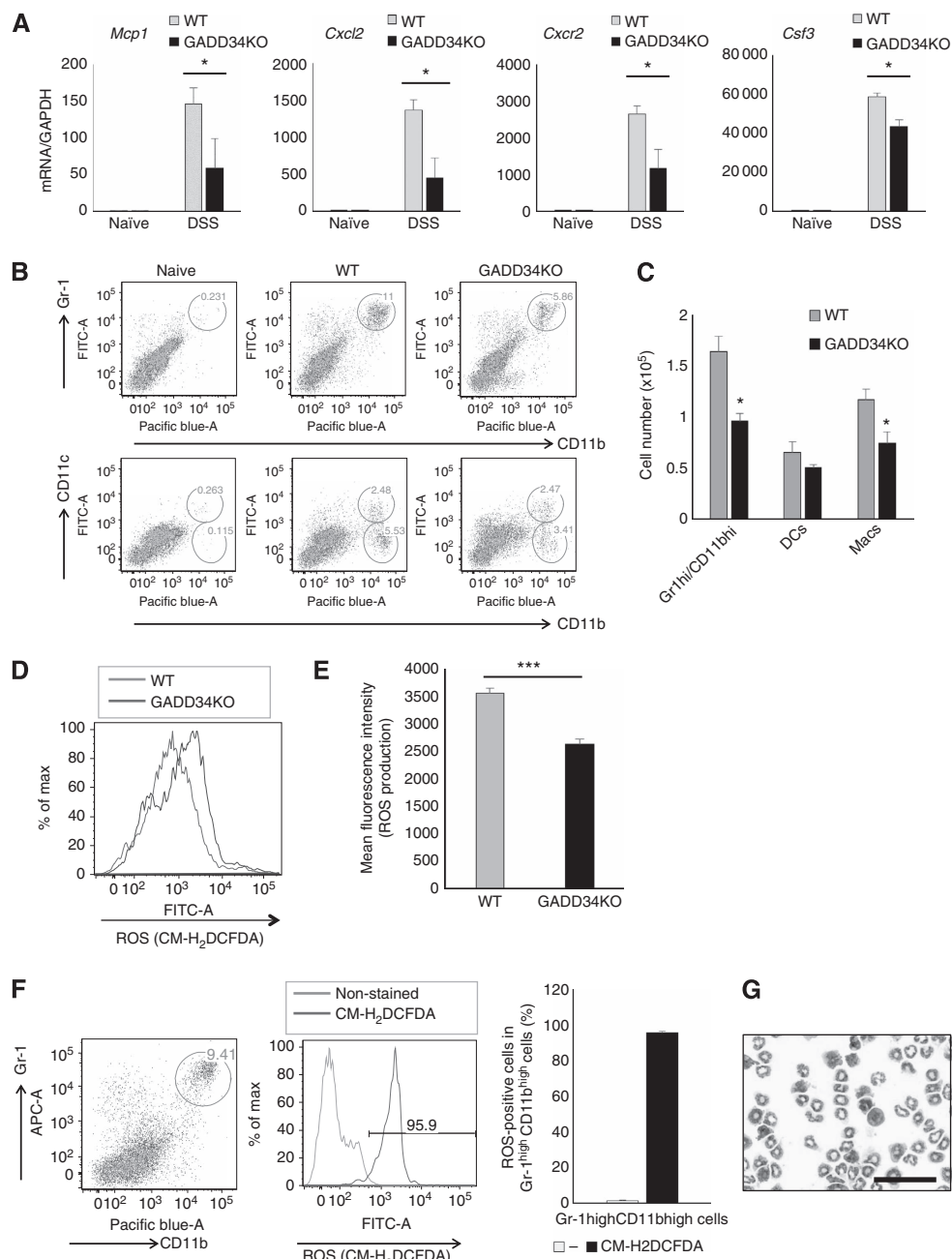


Figure 5. GADD34 enhanced recruitment of neutrophils and macrophages. (A) Gene expression of chemokines (*Mcp1*, *Cxcl2*), a chemokine receptor (*Cxcr2*), and *Csf3* (G-CSF) was analysed in whole distal colon by real-time PCR. Colons were taken from naïve and DSS-treated mice (day 10). Data represent means \pm s.e.m. ($n = 6$). (B) Representative flow-cytometric data plot of lamina propria-infiltrating cells. Lamina propria cells were collected at day 5 of 3% DSS treatment. Data are representative of three experiments (each experiment included two or three mice/group). (C) The numbers of Gr-1^{high}/CD11b^{high} cells, dendritic cells (DCs; CD11b⁺/CD11c⁺), and macrophages (Mac; CD11b⁺/CD11c⁻) were determined by flow-cytometric analysis. Lamina propria cells were collected at day 5 of 3% DSS treatment. Data represent means \pm s.e.m. ($n = 6$). (D and E) ROS production from lamina propria-infiltrating cells at day 5 of 3% DSS treatment was measured by flow-cytometric analysis. Mean fluorescence intensity is shown in (E). Data represent means \pm s.e.m. ($n = 6$). (F) ROS production from Gr-1^{high}/CD11b^{high} cells at day 5 of 3% DSS treatment was measured by flow-cytometric analysis. Statistical graph represents the percentage of ROS-positive cells in the Gr-1^{high}/CD11b^{high} population. Data represent means \pm s.e.m. ($n = 6$). (G) May-Giemsa staining of the Gr-1^{high}/CD11b^{high} population from DSS-treated bone marrow. Scale bar: 50 μ m. * $P < 0.05$, *** $P < 0.001$.

radicals induce TLR-4 signalling (Tun *et al*, 2014). Increased iNOS in human ulcerative colitis (Middleton *et al*, 1993) and colon adenoma has been reported (Ambs *et al*, 1998; Lala and Chakraborty, 2001).

GADD34 has been shown to affect pathogen-induced innate immune responses. Clavarino *et al* (2012) showed that GADD34 expression has positive effects on IL-6 and IFN β production in

dendritic cells stimulated by poly (I:C). In contrast, there are reports that GADD34 expression has negative effects on pro-inflammatory cytokines. Li *et al* (2008) showed that CUEDC2 suppressed the activation of IKK through recruitment of GADD34/PP1 and downregulated NF κ B signalling that in turn suppressed pro-inflammatory cytokine production. Although NF κ B signalling is the main pathway that enhances mRNA expression for pro-

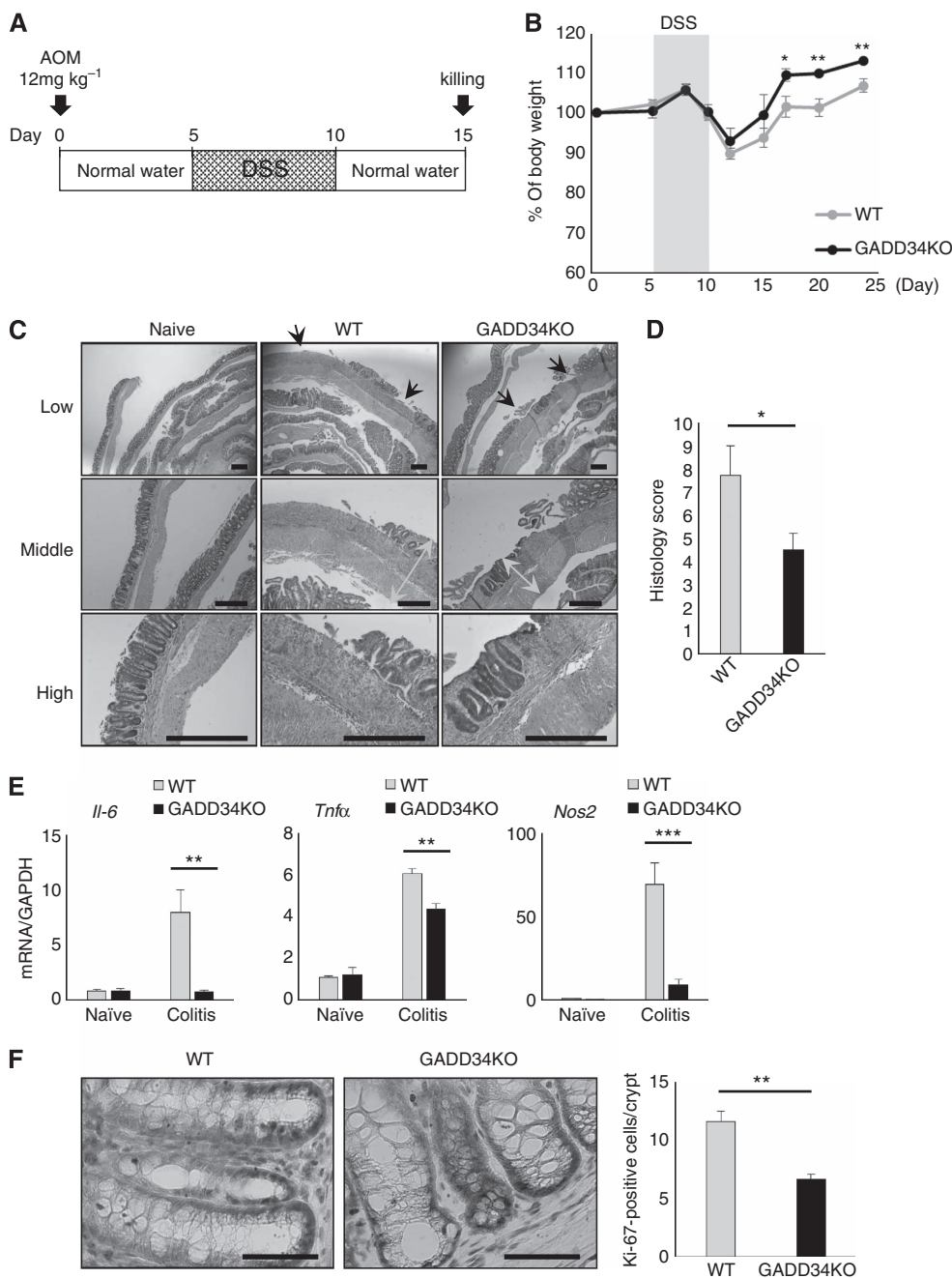


Figure 6. GADD34 promoted epithelial growth after one round of AOM/DSS treatment. **(A)** Schematic diagram of mice treated with AOM/DSS. **(B)** Body weight changes. Body weight at day 0 = 100%. Data represent means \pm s.e.m. ($n = 8$). **(C)** H&E staining of colon tissues taken from AOM/DSS-treated mice at day 15. Black arrows: ulceration; yellow arrows: hyperplasia; blue arrows: infiltration. Scale bar: 300 μ m. **(D)** Semicquantitative scoring of histopathology at day 15 of AOM/DSS treatment. **(E)** Whole colon gene expression of pro-inflammatory mediators (*Il-6*, *Tnfa*, *Nos2/inos*) was analysed by real-time PCR. **(F)** Left: Colonic tissues from AOM/DSS-treated colitis mice (day 15) were collected and immunostained for the proliferation marker Ki-67. Scale bar: 50 μ m. Right: Number of Ki-67-positive cells 10 days after DSS treatment. Data are means \pm s.e.m. ($n = 6$). * $P < 0.05$, ** $P < 0.01$, *** $P < 0.001$. A full color version of this figure is available at the *British Journal of Cancer* journal online.

inflammatory cytokines, we could not detect differences in NF κ B signalling between WT and GADD34KO mice stimulated with DSS (Figure 3D and E). We detected higher expression of MAPK signalling pathways in WT mice than in GADD34KO mice (Figure 3F and G).

ER stress is linked to the pathogenesis of IBD (Shkoda *et al*, 2007; Cao *et al*, 2013). However, our data revealed that DSS or AOM/DSS treatment did not clearly enhance p-eIF2 α expression in either WT or GADD34KO colons (Supplementary Figures 2c and 3a). Expression of CHOP or ATF4 was not increased by DSS treatment in either WT or GADD34KO colons (Supplementary Figure 3b).

Recently, it was documented that GADD34KO mice showed earlier recovery than WT mice in a skin wound healing model (Liu *et al*, 2014). They demonstrated that GADD34 inhibited myofibroblast differentiation through its inhibition of the Smad3-dependent TGF- β signal pathway and by promoting apoptosis by activating the caspase-3 pathway. However, we could not detect differences in apoptosis, p-smad2/3, or TGF- β expression or α -SMA-positive areas between WT and GADD34KO mice after DSS treatment (Supplementary Figure 4a–e). Instead, DSS treatment induced stronger recruitment of macrophages and neutrophils to damaged colon tissues in WT than in GADD34KO

mice, and those cells produced pro-inflammatory cytokines, including IL-6 (Figure 5B and C).

Taken together, DSS treatment induced GADD34 expression that paralleled the expression of inflammatory cytokines and iNOS. In particular, IL-6/STAT3 signalling and JNK and ERK signalling were enhanced. Thus, GADD34 deficiency prevented the activation of IL-6/STAT3 signalling and signalling by JNK and ERK. As a result, the levels of pro-inflammatory cytokines were lower, and iNOS production was reduced, as were inflammatory responses and epithelial growth in AOM/DSS-induced colitis. This study demonstrated that GADD34 promoted AOM/DSS-induced carcinogenesis by enhancing IL-6 production from myeloid cells and subsequent STAT3 activation in epithelial cells.

ACKNOWLEDGEMENTS

We thank N Oiwa for administrative assistance and M Tanaka for technical support of flow-cytometric analysis and cell sorting. This work was supported by Grants-in-Aid for Scientific Research from Japan Society for the Promotion of Science: Grant numbers 25293166, 24500852, and 26870257.

CONFLICT OF INTEREST

The authors declare no conflict of interest.

AUTHOR CONTRIBUTIONS

YT, SI, and KI contributed to data acquisition, study design and paper authorship; RO, NC, and NN contributed to technical support.

REFERENCES

- Abreu MT (2010) Toll-like receptor signalling in the intestinal epithelium: how bacterial recognition shapes intestinal function. *Nat Rev Immunol* **10**(2): 131–144.
- Ambis S, Merriam WG, Bennett WP, Felley-Bosco E, Ogunfusika MO, Oser SM, Klein S, Shields PG, Billiar TR, Harris CC (1998) Frequent nitric oxide synthase-2 expression in human colon adenomas: implication for tumor angiogenesis and colon cancer progression. *Cancer Res* **58**(2): 334–341.
- Arumugam M, Raes J, Pelletier E, Le Paslier D, Yamada T, Mende DR, Fernandes GR, Tap J, Bruls T, Batto JM, Bertalan M, Borruel N, Casellas F, Fernandez L, Gautier L, Hansen T, Hattori M, Hayashi T, Kleerebezem M, Kurokawa K, Leclerc M, Levenez F, Manichanh C, Nielsen HB, Nielsen T, Pons N, Poulain J, Qin J, Sicheritz-Ponten T, Tims S, Torrents D, Ugarte E, Zoetendal EG, Wang J, Guarner F, Pedersen O, de Vos WM, Brunak S, Doré J, Antolin M, Artiguenave F, Blottiere HM, Almeida M, Brechot C, Cara C, Chervaux C, Cultrone A, Delorme C, Denariac G, Dervyn R, Foerstner KU, Friss C, van de Guchte M, Guedon E, Haimet F, Huber W, van Hylckama-Vlieg J, Jamet A, Juste C, Kaci G, Knol J, Lakhdari O, Layec S, Le Roux K, Maguin E, Mérieux A, Melo Minardi R, M'rimi C, Muller J, Oozeer R, Parkhill J, Renault P, Rescigno M, Sanchez N, Sunagawa S, Torrejon A, Turner K, Vandemeulebrouck G, Varela E, Winogradsky Y, Zeller G, Weissenbach J, Ehrlich SD, Bork P. MetaHit Consortium (2011) Enterotypes of the human gut microbiome. *Nature* **473**(7346): 174–180.
- Atreya R, Neurath MF (2005) Involvement of IL-6 in the pathogenesis of inflammatory bowel disease and colon cancer. *Clin Rev Allergy Immunol* **28**(3): 187–196.
- Becker C, Fantini MC, Schramm C, Lehr HA, Wirtz S, Nikolaev A, Burg J, Strand S, Kiesslich R, Huber S, Ito H, Nishimoto N, Yoshizaki K, Kishimoto T, Galle PR, Blessing M, Rose-John S, Neurath MF (2004) TGF-beta suppresses tumor progression in colon cancer by inhibition of IL-6 trans-signaling. *Immunity* **21**(4): 491–501.
- Cao SS, Zimmermann EM, Chuang BM, Song B, Nwokoye A, Wilkinson JE, Eaton KA, Kaufman RJ (2013) The unfolded protein response and chemical chaperones reduce protein misfolding and colitis in mice. *Gastroenterology* **144**(5): 989–1000.e6.
- Clavirino G, Cláudio N, Dalet A, Terawaki S, Couderc T, Chasson L, Ceppi M, Schmidt EK, Wenger T, Lecuit M, Gatti E, Pierre P (2012) Protein phosphatase 1 subunit Ppp1r15a/GADD34 regulates cytokine production in polyinosinic:polycytidylic acid-stimulated dendritic cells. *Proc Natl Acad Sci USA* **109**(8): 3006–3011.
- Dipple A (1995) DNA adducts of chemical carcinogens. *Carcinogenesis* **16**(3): 437–441.
- Fornace AJ, Alamo I, Hollander MC (1988) DNA damage-inducible transcripts in mammalian cells. *Proc Natl Acad Sci USA* **85**(23): 8800–8804.
- Greten FR, Eckmann L, Greten TF, Park JM, Li ZW, Egan LJ, Kagnoff MF, Karin M (2004) IKKbeta links inflammation and tumorigenesis in a mouse model of colitis-associated cancer. *Cell* **118**(3): 285–296.
- Grivennikov S, Karin E, Terzic J, Mucida D, Yu GY, Vallabhapurapu S, Scheller J, Rose-John S, Cheroutre H, Eckmann L, Karin M (2009) IL-6 and Stat3 are required for survival of intestinal epithelial cells and development of colitis-associated cancer. *Cancer Cell* **15**(2): 103–113.
- Gu M, Ouyang C, Lin W, Zhang T, Cao X, Xia Z, Wang X (2014) Phosphatase holoenzyme PP1/GADD34 negatively regulates TLR response by inhibiting TAK1 serine 412 phosphorylation. *J Immunol* **192**(6): 2846–2856.
- Harding HP, Zhang Y, Scheuner D, Chen JJ, Kaufman RJ, Ron D (2009) Ppp1r15 gene knockout reveals an essential role for translation initiation factor 2 alpha (eIF2alpha) dephosphorylation in mammalian development. *Proc Natl Acad Sci USA* **106**(6): 1832–1837.
- Herrinton LJ, Liu L, Levin TR, Allison JE, Lewis JD, Velayos F (2012) Incidence and mortality of colorectal adenocarcinoma in persons with inflammatory bowel disease from 1998 to 2010. *Gastroenterology* **143**(2): 382–389.
- Hollander MC, Zhan Q, Bae I, Fornace AJ (1997) Mammalian GADD34, an apoptosis- and DNA damage-inducible gene. *J Biol Chem* **272**(21): 13731–13737.
- Ito S, Tanaka Y, Oshino R, Aiba K, Thanasegaran S, Nishio N, Isobe K (2015) GADD34 inhibits activation-induced apoptosis of macrophages through enhancement of autophagy. *Sci Rep* **5**: 8327.
- Jemal A, Center MM, DeSantis C, Ward EM (2010) Global patterns of cancer incidence and mortality rates and trends. *Cancer Epidemiol Biomarkers Prev* **19**(8): 1893–1907.
- Kishimoto T (2005) Interleukin-6: from basic science to medicine—40 years in immunology. *Annu Rev Immunol* **23**: 1–21.
- Kojima E, Takeuchi A, Haneda M, Yagi A, Hasegawa T, Yamaki K, Takeda K, Akira S, Shimokata K, Isobe K (2003) The function of GADD34 is a recovery from a shutoff of protein synthesis induced by ER stress: elucidation by GADD34-deficient mice. *FASEB J* **17**(11): 1573–1575.
- Lala PK, Chakraborty C (2001) Role of nitric oxide in carcinogenesis and tumour progression. *Lancet Oncol* **2**(3): 149–156.
- Li HY, Liu H, Wang CH, Zhang JY, Man JH, Gao YF, Zhang PJ, Li WH, Zhao J, Pan X, Zhou T, Gong WL, Li AL, Zhang XM (2008) Deactivation of the kinase IKK by CUEDC2 through recruitment of the phosphatase PP1. *Nat Immunol* **9**(5): 533–541.
- Liu L, Nishio N, Ito S, Tanaka Y, Isobe K (2014) Negative regulation of GADD34 on myofibroblasts during cutaneous wound healing. *Biomed Res Int* **2014**: 137049.
- Mantovani A, Allavena P, Sica A, Balkwill F (2008) Cancer-related inflammation. *Nature* **454**(7203): 436–444.
- Mengedorf T, Althausen S, Oberndorfer I, Paschen W (2001) Response of neurons to an irreversible inhibition of endoplasmic reticulum Ca(2+) -ATPase: relationship between global protein synthesis and expression and translation of individual genes. *Biochem J* **356**(Pt 3): 805–812.
- Mesman AW, Zijlstra-Willems EM, Kaptein TM, de Swart RL, Davis ME, Ludlow M, Duprex WP, Gack MU, Gringhuis SI, Geijtenbeek TB (2014) Measles virus suppresses RIG-I-like receptor activation in dendritic cells via DC-SIGN-mediated inhibition of PP1 phosphatases. *Cell Host Microbe* **16**(1): 31–42.
- Middleton SJ, Shorthouse M, Hunter JO (1993) Increased nitric oxide synthesis in ulcerative colitis. *Lancet* **341**(8843): 465–466.
- Novoa I, Zeng H, Harding HP, Ron D (2001) Feedback inhibition of the unfolded protein response by GADD34-mediated dephosphorylation of eIF2alpha. *J Cell Biol* **153**(5): 1011–1022.

- Novoa I, Zhang Y, Zeng H, Jungreis R, Harding HP, Ron D (2003) Stress-induced gene expression requires programmed recovery from translational repression. *EMBO J* **22**(5): 1180–1187.
- Shkoda A, Ruiz PA, Daniel H, Kim SC, Rogler G, Sartor RB, Haller D (2007) Interleukin-10 blocked endoplasmic reticulum stress in intestinal epithelial cells: impact on chronic inflammation. *Gastroenterology* **132**(1): 190–207.
- Tun X, Yasukawa K, Yamada K (2014) Involvement of nitric oxide with activation of Toll-like receptor 4 signaling in mice with dextran sodium sulfate-induced colitis. *Free Radic Biol Med* **74**: 108–117.
- Yu H, Pardoll D, Jove R (2009) STATs in cancer inflammation and immunity: a leading role for STAT3. *Nat Rev Cancer* **9**(11): 798–809.
- Zaki MH, Vogel P, Malireddi RK, Body-Malapel M, Anand PK, Bertin J, Green DR, Lamkanfi M, Kanneganti TD (2011) The NOD-like receptor NLRP12 attenuates colon inflammation and tumorigenesis. *Cancer Cell* **20**(5): 649–660.
- Zhan Q, Lord KA, Alamo I, Hollander MC, Carrier F, Ron D, Kohn KW, Hoffman B, Liebermann DA, Fornace AJ (1994) The gadd and MyD genes define a novel set of mammalian genes encoding acidic proteins that synergistically suppress cell growth. *Mol Cell Biol* **14**(4): 2361–2371.

This work is published under the standard license to publish agreement. After 12 months the work will become freely available and the license terms will switch to a Creative Commons Attribution-NonCommercial-Share Alike 4.0 Unported License.

Supplementary Information accompanies this paper on British Journal of Cancer website (<http://www.nature.com/bjc>)